

Communication

1.73 kW CW Amplification ASE Source Based on Yb³⁺ Ions-Doped All-Fiber System

Xin Li ^{1,2,3,*}, Zhe Zhang ³, Xinyang Xu ⁴, Junjie Liu ^{1,2} and Xiaolei Bai ^{1,2}

¹ Institute of Laser and Optoelectronics, College of Precision Instrument and Optoelectronics Engineering, Tianjin University, Tianjin 300072, China

² Key Laboratory of Optoelectronic Information Science and Technology, Ministry of Education, Tianjin University, Tianjin 300072, China

³ Tianjin Jinhang Research Institute of Technical Physics, Tianjin 300381, China

⁴ Science and Technology on Electro-Optical Information Security Control Laboratory, Tianjin 300308, China

* Correspondence: lixintjuht@163.com

Abstract: The all-fiber ASE source is an intriguing tool in the fields of super-fluorescence detection, coherent measurement and spectrum analysis technology. We experimentally demonstrate a continuous all-fiber amplified spontaneous emission (ASE) source based on a master-oscillator power amplifier (MOPA) system, which aims at achieving high power and frequency stability. The seed source is homemade ASE low power super-fluorescence source with 200 mW. The system employs large-mode-area Yb³⁺-doped double-clad fiber (LMA-DCF), and the maximum power can reach 1.73 kW at a center wavelength of 1079.36 nm, and can maintain an optical-to-optical conversion efficiency of 79.13%. During 30 min of real-time monitoring, the ASE source system did not generate a nonlinear effect, and power fluctuation was less than 2%.

Keywords: all-fiber; continuous wave (CW); super-fluorescence; ASE source; kW laser



Citation: Li, X.; Zhang, Z.; Xu, X.; Liu, J.; Bai, X. 1.73 kW CW Amplification ASE Source Based on Yb³⁺ Ions-Doped All-Fiber System. *Photonics* **2023**, *10*, 81. <https://doi.org/10.3390/photonics10010081>

Received: 7 December 2022

Revised: 3 January 2023

Accepted: 5 January 2023

Published: 10 January 2023



Copyright: © 2023 by the authors. Licensee MDPI, Basel, Switzerland. This article is an open access article distributed under the terms and conditions of the Creative Commons Attribution (CC BY) license (<https://creativecommons.org/licenses/by/4.0/>).

1. Introduction

Low-coherence bandwidth sources show unparalleled superiority in applications of fiber sensing and detection [1]. Additionally, high-power amplified spontaneous emission (ASE) sources based on rare-earth-doped fibers show numerous benefits, such as temporal stability, high thermal stability and short coherence length. Their excellent performances make them suitable for optical coherence tomography, low-coherence interference and optical fiber sensing [2,3]. Furthermore, compared with commercial broadband super luminescent diodes (SLD), ASE sources have the advantages of excellent beam quality and high conversion efficiency [4]. In doped fibers, with increasing fiber-stimulated ion ASE, the particle numbers display a sharp inversion at the threshold, and the source produces a super-fluorescence phenomenon. The longitudinal mode of the super-fluorescence source covers a wide range, which perform stable in some spectrum amplifying. In a great deal of laser technology research, super-fluorescence sources (ASE sources) are receiving extensive attention as seed sources.

The ytterbium-doped fiber (YDF) ASE source possesses characteristics of fluorescence and lasers in rare-earth-doped fibers. Ytterbium-doped fiber (YDF) has a wide range of the oscillating spectrum, especially in the C band of high work efficiency [5]. YDF adopts the structure of large-mode-area (LMA) fibers to improve laser output power, with a LD pump of high power and high brightness, so that the ASE source output power can attain an average (or higher) level [6–8]. In recent years, many works of research investigating high-power ASE sources have been demonstrated. Relevant research has shown that 1 μm bands were conducive to generating high-power ASE sources. The researchers mainly extracted super-fluorescence sources from ASE sources or extended spectral line widths by ASE seed sources. Wang et al. researched the wavelength range of 1 μm, and utilized

combinatorial methods of multi-mode bias fibers and a double-head super-fluorescence source, which had an output power of 110 W and an optical conversion efficiency of 68%, a measured beam quality factor (M^2) of 1.6 and a full width at half maximum (FWHM) of 40 nm. The central wavelength was 1063 nm and the spectral bandwidth range covered 1032~1120 nm [9]. Furthermore, they also improved the efficiency of ytterbium-doped double-clad helical core fibers in super-fluorescence (non-laser) structures; the system output power was 107 W with a highest optical conversion efficiency of 76% at 1075 nm, and the spectral bandwidth was 1030~1160 nm. The corresponding FWHM was 37 nm and the measured beam quality factor (M^2) was 2.8; they also achieved the effect of suppressing laser helical core fibers [10]. In 2007, Wang et al. researched fluorescent seed sources in the two-stage MOPA amplification system, whose minimum seed power was 10 mW. The output power was 106 W with an optical conversion efficiency of 67% at 1030 nm. The spectral bandwidth covered 1035~1100 nm, with a FWHM of 21 nm and a beam quality factor (M^2) of less than 1.1 [11]. In 2011, Schmidt et al. built a three-stage MOPA system with a fluorescence source. The fluorescent seed source was 400 mW, and the maximum output power was 697 W, with an optical conversion efficiency of 69% at 1030 nm. The output's spectral bandwidth was 1030~1160 nm and the beam quality factor (M^2) was less than 1.34 [12]. In 2012, Cao et al. reported a super-fluorescence source generated by an ytterbium-doped fiber amplifier based on an all-fiber MOPA structure. The system's super-fluorescent seed source was 3 W, and the maximum output power was 102 W with an optical conversion efficiency of 70% at 1050 nm. The spectral bandwidth was 1020~1130 nm and the FWHM was 21 nm [13]. In 2014, Liu et al. constructed an all-fiber super-fluorescence source with MOPA-doped thulium, whose output power was 100 W, and whose optical conversion efficiency was 60% at 1985 nm. The spectral bandwidth was 1935~2075 nm, corresponding to a FWHM of 25 nm [14]. In 2015, Huang et al. designed a two-stage MOPA all-fiber system, whose maximum super-fluorescence seed source output was 0.8 W. The whole system's output power was 1.01 kW, and the optical conversion efficiency was 80.3% at 1074.4 nm. The spectral bandwidth was 1040~1100 nm, corresponding to a FWHM of 8.1 nm and a beam quality factor (M^2) less than 1.8 [15]. In 2015, Huang et al. designed a three-level MOPA polarization-maintained all-fiber (PMF) super-fluorescence source system, with a system seed source of 30 mW. The system's maximum output power was 1.42 kW, with an optical conversion efficiency of 80% at 1074 nm. The spectral bandwidth was 1050~1100 nm, with a FWHM of 11 nm and a beam quality factor (M^2) of 1.14 [16]. In 2016, An et al. established an all-fiber single-stage amplification super-fluorescence source, with an output power of 184 W and an optical efficiency of 78% at 1055 nm. The ASE spectra range was 1030~1100 nm and the FWHM was larger than 20 nm [17]. In 2020, Li et al. established an all-fiber MOPA super-fluorescence source, with a seed source of 2.23 W. The system's output power was 1 kW with an optical efficiency of 75% at 1055 nm. The ASE spectrum range was 1045~1085 nm and the beam quality factor (M^2) could attain a value of 1.40 [18]. In 2021, Wu et al. established a super-fluorescence source with Yb-Raman fiber amplifiers; the system's output power was 1.16 kW and optical efficiency was 72.5% at 1120 nm. The ASE spectrum was within the range of 1045~1085 nm, and the FWHM was 4.77 nm [19].

In this work, we developed a high-power ASE super-fluorescent source utilizing ASE spectral properties. We built an all-fiber continuous ASE source based on the MOPA system. The seed source used a homemade ASE low-power super-fluorescence source (200 mW). The seed source was amplified through multi-stage 975 nm pumps, with a maximum continuous power of 1.73 kW and a FWHM of 3.7 nm at 1079.36 nm. The system had no nonlinear effects or high-order mode interference. Based on the measurements, the ASE source system's output power maintained a stable state, and the beam quality factor (M^2) was less than or equal to 1.763.

2. Experimental Setup

As shown in Figure 1, the experimental setup of the ASE source is set up based on MOPA system. To obtain a super-fluorescence source with highly efficient excitation and as table low power output, we generated an ASE seed source by the backward pumping method. In the experiment, we employed a 5 m homemade ytterbium-doped fiber (LMA-YDF-10/130); it served as the gain fiber of the laser seed with an absorption of 4.57 dB/m at 975 nm, and the NA of the core and cladding was 0.075 and 0.46, respectively. In order to reduce the back-end reflection entering the gain fiber and restrain parasitic oscillation, we adopted an incidence angle of 8°. The seed wasa homemade ASE source with a maximum average power of 200 mW, which was amplified by a four-stage MOPA system. In the first and second pre-amplifier, two sections of 5 m ytterbium-doped fiber (LMA-YDF-15/130) were pumped by a 975 nm multimode laser diode (LD) through a (2 + 1) × 1 coupler. The cladding absorption efficiency was 5.30 dB/m at 975 nm, and the NA of the core and the cladding was 0.08 and 0.46, respectively. In the third pre-amplifier, we adopted an ytterbium-doped fiber (LMA-YDF 20/130) of 10 m, which had an average absorption of 8.10 dB/m at 975 nm and was equipped with 0.08 NA and 0.46 cladding. An optical isolator was inserted to block the back-reflection in the system. The power monitors detected the power of the signal source in real time, and minimized damage to the signal source in the amplification process. The Mode Field Adaptor (MFA) enhanced the efficiency of mode matching, and restrained high-order modes. The main amplifier utilized 20 m of LMA-YDF 20/400 (Nufern Company, East Granby, CT, USA), and the NA of the core and cladding was 0.06 and 0.46, respectively. The average absorption coefficient can be quantified as 1.27 dB/m at 975 nm. The homemade CLS (cladding light stripper) was welded after the active fiber, which absorbed the residual pump light from cladding. After the signal light was output through the CLS, it was connected to the 0.5 m-long passive fiber and output to the space through a collimator. The whole system was cooled by water-cooling to improve the laser performance.

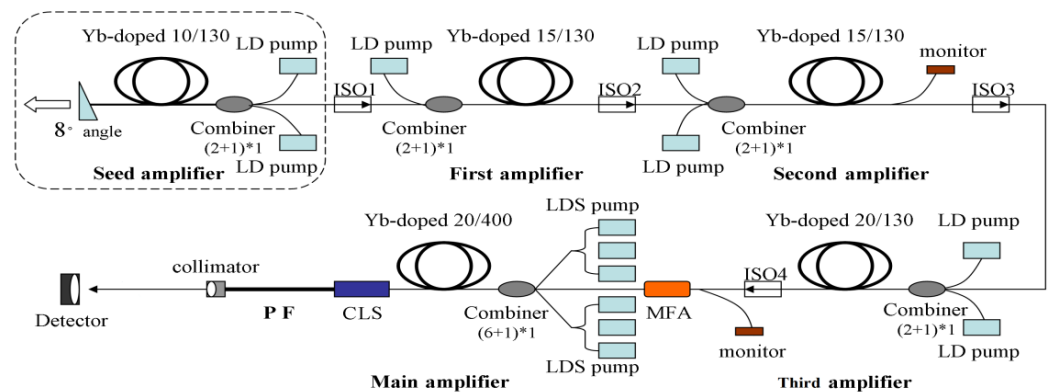


Figure 1. All-fiber amplifier system of ASE source.

3. Experimental Results and Discussion

In the experiment, we developed a low-power ASE seed. Short gain fibers and low pump power were applied to improve the stability of output power. The seed power gradually increased during the ASE magnifying process, and the minimum super-fluorescence output power was 200 mW. The spectrum of ASE super-fluorescence seed was detected as shown in Figure 2. The super-fluorescence spectral width was about 1048~1085 nm. The central wavelength of the ASE seed was 1070 nm and the FWHM was 28 nm. Due to the 8° angle at the end of the Yb-doped fiber, self-excited oscillation was not observed.

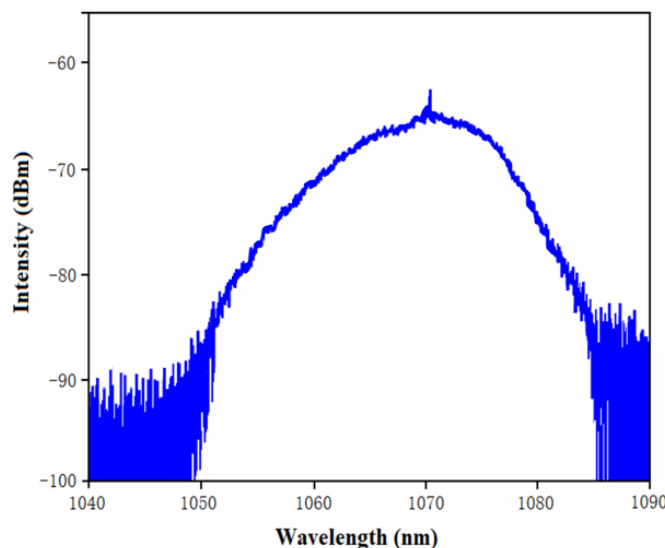


Figure 2. Spectrum of ASE super-fluorescence seed.

When the pump power was 245 W, the pre-amplifier output power was about 128 W. To maintain the stability of the amplification spectrum, the low-power 5 W pump source was used in the first stage of amplification. In the three-stage pre-amplification spectrum, with increases in pump power and output power, the central wavelength appeared to display a red-shift (frequency-shift) phenomenon, as shown in Figure 3. This phenomenon also appeared in the power amplification stage (main stage amplification). Interestingly, during each stage of pre-amplification, we also discovered that the FWHM was gradually reduced from 25 nm to 13 nm, and the FWHM was reduced to 3.7 nm at the power amplification stage (main stage amplification). The central wavelength and FWHM versus different output powers were altered as shown in Figure 4. With increasing output power, the central wavelength kept shifting and increasing. After the power increased to 1.73 kW, the central wavelength tended to be stable, and the FWHM tended to decrease with increasing output power. In the output process of the power amplification stage (main stage amplification), the FWHM showed a relatively stable state.

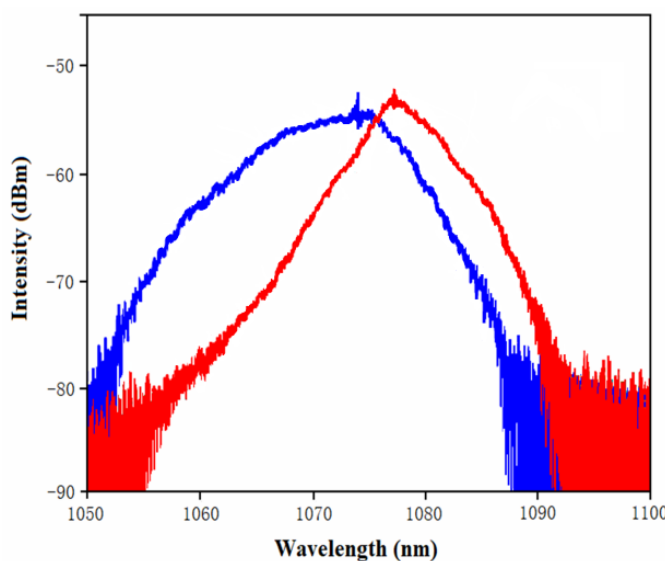


Figure 3. The spectrum’s red-shift trend.

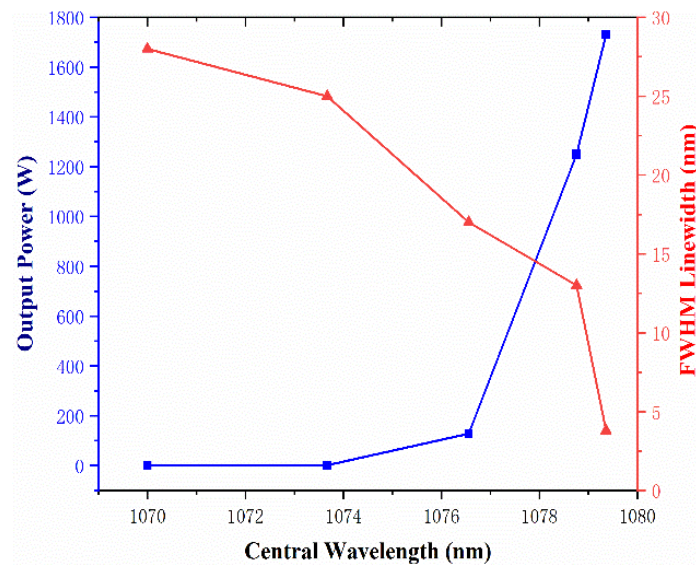


Figure 4. Variation trend of output power and FWHM.

Due to the spectrum's red-shift (central wavelength shift) trend and the FWHM narrowing, first of all, with increasing LD pump drive current, the pump's working temperature increased, and the 975 nm pump's wavelength appeared to be frequency-shifted (976~980 nm), so the gain fiber absorption pump's wavelength was altered. The secondly, with increasing optical amplification power, the internal temperature of the fiber increases accordingly. The gain fiber temperature of the power amplification stage was, again, higher than the gain fiber temperature of the pre-amplification stage, while the optical absorption of the short-wavelength signal met the fiber temperature under certain conditions. With a gradual increase in temperature, the optical absorption of the long-wavelength signal was dominant. With an increase in optical frequency, the center of the gain spectrum moved to the long wavelength, and the line width gradually became narrower. Finally, as the gain of doped particles in the gain fiber increased, a number of particles showed active inversion and interacted with lattice thermal phonons to produce an energy exchange. As the temperature increased, the corresponding changes were manifested in the frequency spectrum and frequency drift of the central wavelength.

As shown in Figure 5, the output power linearly increased with pump power. The maximum output power could reach 1.73 kW with a pump power of 2.18 kW, corresponding with an optical-to-optical efficiency of 79.13%. With a gradual increase in ASE source power, the frequency shift of the output spectrum kept changing. The peak power of the central wavelength was concentrated at 1079.36 nm, and the peak power of the system was 1.73 kW, as shown in Figure 6. To verify the stability of the output power, the system operated for 30 min, and the experimental results were detected in real time. The output power instability was less than 2%, as shown in Figure 7a,b. The continuous all-fiber ASE source amplification system did not display self-pulsation, relaxation oscillation or power inversion phenomena. The experimental results indicated that it was feasible to further improve the pumping power and output power via controlling the stable output of the amplifiers at all stages.

In the experiments, we measured the beam quality of the 1.73 kW ASE source. The measuring method adopted the evaluation criteria commonly used in the laser industry [20,21]. We established a nonlinear fitting function for the optical transmission process and used the sampled data to fit the function [22,23]. As shown in Figure 8, the beam quality factor (M^2) was 1.649 in the x-direction and 1.763 in the y-direction.

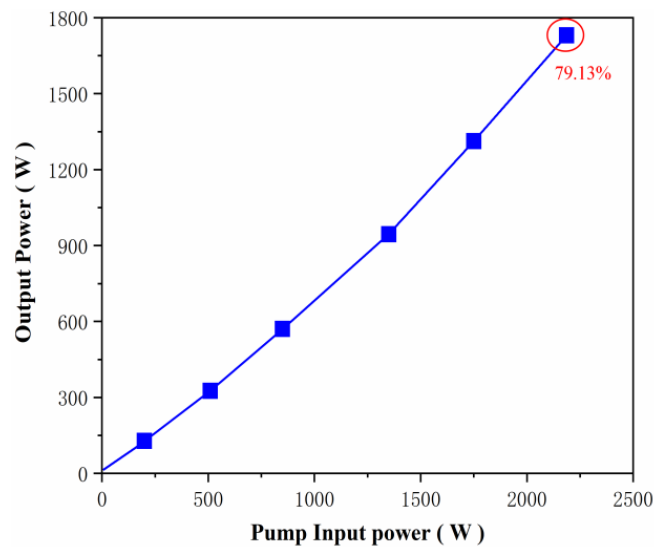


Figure 5. Optical-to-optical conversion efficiency.

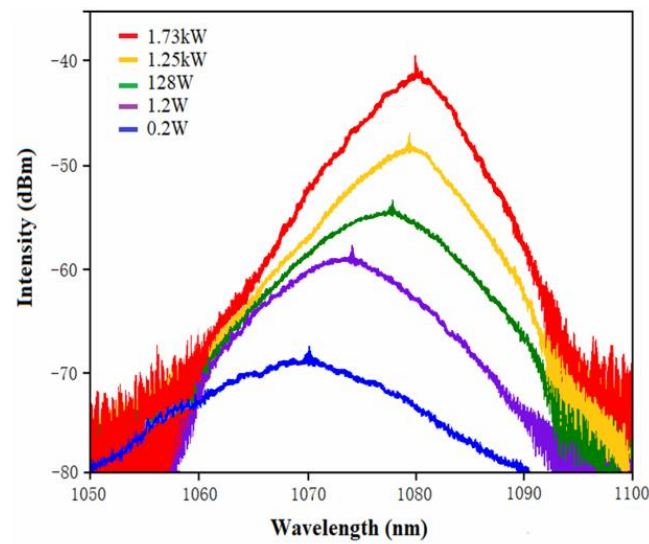


Figure 6. Main spectral line frequency-shift process.

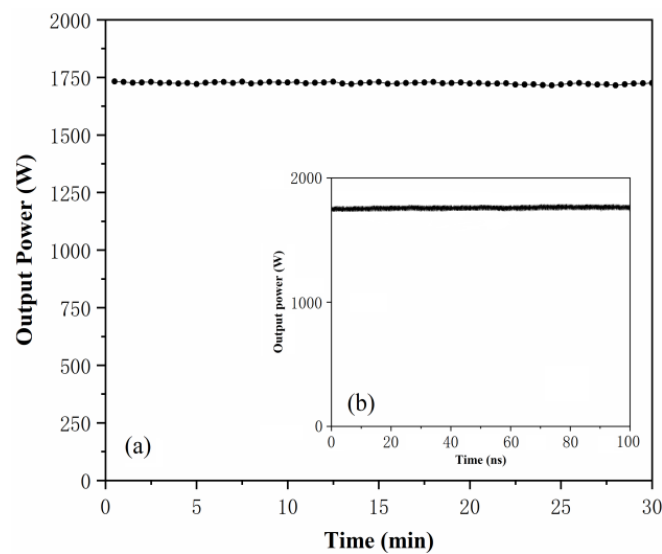


Figure 7. (a) Continuous output power stability. (b) Stable output of power in the nanosecond ranges).

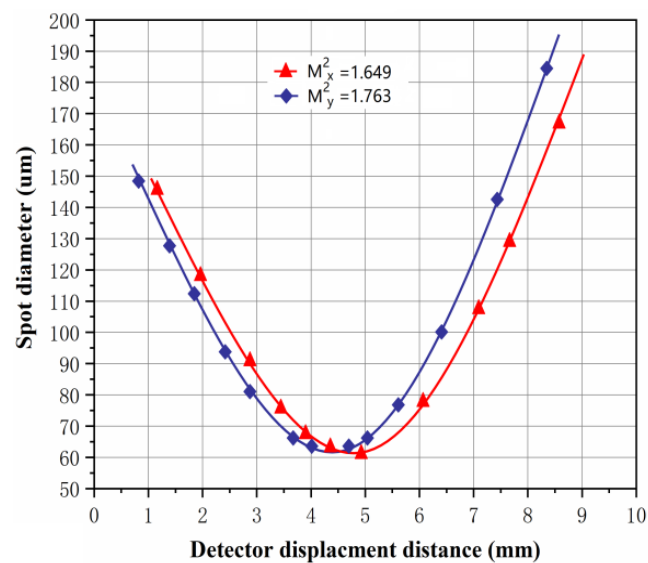


Figure 8. Beam quality factor (M^2) of ASE source at the output power of 1.73 kW.

4. Conclusions

In this paper, we demonstrate a continuous high-power all-fiber ASE source based on the MOPA system. The seed source is a homemade ASE source (super-fluorescence) with a 200 mW power output. Through the four-stage MOPA system, the maximum output power can reach 1.73 kW, which corresponds to an optical-to-optical conversion efficiency of 79.13%. The central wavelength is 1079.36 nm and the FWHM is 3.7 nm at 1.73 kW output power. We analyze the frequency-shift phenomenon of the center wavelength and the bandwidth's narrowing effect during ASE seed source amplification. The system suppresses higher-order mode disturbances and nonlinear effects. The output power fluctuation is less than 2%. The beam quality factor (M^2) is 1.649 in the x-direction and 1.763 in the y-direction. The system can be extensively used in the fields of super-fluorescence detection, material composition analysis, coherent measurement, fiber sensing and spectral analysis.

Author Contributions: Conceptualization, X.L., Z.Z., X.X. and J.L.; methodology, X.L., Z.Z., X.X. and J.L.; software, X.L.; validation, X.L. and Z.Z.; formal analysis, X.L., Z.Z. and X.X.; investigation, X.L. and Z.Z.; resources, X.L. and X.B.; data curation, X.L. and Z.Z.; writing—original draft preparation, X.L., Z.Z. and X.X.; writing—review and editing, X.L. and X.X.; visualization, X.L., Z.Z. and X.X.; supervision, X.L.; project administration, X.L. All authors have read and agreed to the published version of the manuscript.

Funding: This paper was sponsored by the National Natural Science Foundation of China (NSFC) (Grants No.61775163).

Institutional Review Board Statement: Not applicable.

Informed Consent Statement: Not applicable.

Data Availability Statement: The data used to support the findings of this study are available from the corresponding author upon request.

Conflicts of Interest: The authors declare no conflict of interest.

References

1. Wysocski, P.F.; Digonnet, M.J.; Kim, B.Y.; Shaw, H.J. Characteristics of Er^{3+} -doped super-fluorescent fiber source for interferometric sensor application. *J. Light Wave Technol.* **1994**, *12*, 550–567. [[CrossRef](#)]
2. Digonnet, M.J.F. Theory of superfluorescent fiber lasers. *J. Light Wave Technol.* **1986**, *4*, 1631–1639. [[CrossRef](#)]
3. Fercher, A.F.; Drexler, W.; Hitzhberger, C.K. Optical coherence tomography principles and applications. *Rep. Prog. Phys.* **2003**, *66*, 239–303. [[CrossRef](#)]

4. Martin-Lopez, S.; Gonzalez-Herraez, M.; Carrasco-Sanz, A.; Vanholsbeeck, F.; Coen, S.; Fernandez, H.; Solis, J.; Corredera, P.; Hernanz, M.L. Broadband spectrally flat and high power density fbeam source for fibre sensing purposes. *Meas. Sci. Technol.* **2006**, *17*, 1014–1019. [[CrossRef](#)]
5. Kurkov, A.S. Oscillation spectral range of Yb-doped fiber lasers. *Laser Phys. Lett.* **2007**, *4*, 93–102. [[CrossRef](#)]
6. Stiles, E. New developments in IPG fiber laser technology. In Proceedings of the 5th International Workshop on Fiber Lasers, Dresden, Germany, 30 September 2009.
7. He, B.; Zhou, J.; Lou, Q.; Xue, Y.; Li, Z.; Wang, W.; Dong, J.; Wei, Y.; Chen, W. 1.75 KW continuous-wave output fiber laser using homemade ytterbium-doped large-core fiber. *Microw. Opt. Technol. Lett.* **2010**, *52*, 1668–1671. [[CrossRef](#)]
8. Wirth, C.; Schmidt, O.; Tsybin, I.; Schreiber, T.; Peschel, T.; Brückner, F.; Clausnitzer, T.; Limpert, J.; Eberhardt, R.; Tünnermann, A.; et al. 2KW incoherent beam combining of four narrow-linewidth photonic crystal fiber amplifiers. *Opt. Express* **2009**, *17*, 1178–1183. [[CrossRef](#)] [[PubMed](#)]
9. Wang, P.; Sahu, J.K.; Clarkson, W.A. 110 W double-ended ytterbium-doped fiber super-fluorescent source with $M^2 = 1.6$. *Opt. Lett.* **2006**, *31*, 3116–3118. [[CrossRef](#)] [[PubMed](#)]
10. Wang, P.; Sahu, J.K.; Clarkson, W.A. High-power broadband ytterbium-doped helical-core fiber super-fluorescent source. *IEEE Photon. Technol. Lett.* **2007**, *19*, 300–302. [[CrossRef](#)]
11. Wang, P.; Clarkson, W.A. High-power, single-mode, linearly polarized, ytterbium-doped fiber super-fluorescent source. *Opt. Lett.* **2007**, *32*, 2605–2607. [[CrossRef](#)] [[PubMed](#)]
12. Schmidt, O.; Rekas, M.; Wirth, C.; Rothhardt, J.; Rhein, S.; Kliner, A.; Strecker, M.; Schreiber, T.; Limpert, J.; Eberhardt, R.; et al. High power narrow-band fiber-based ASE source. *Opt. Express* **2011**, *19*, 4421–4427. [[CrossRef](#)] [[PubMed](#)]
13. Cao, Y.; Liu, J.; Wang, K.; Wang, P. All-fiber hundred-Watt-level broadband ytterbium-doped double cladding fiber super-fluorescent source. *Chin. J. Lasers* **2012**, *39*, 0802008. [[CrossRef](#)]
14. Liu, J.; Liu, K.; Tan, F.; Wang, P. High-power thulium-doped all-fiber super-fluorescent sources. *IEEE J. Sel. Top. Quantum Electron.* **2014**, *20*, 3100306.
15. Xu, J.M.; Huang, L.J.; Chen, J.B. 1.01 KW super-fluorescent source in all-fiberized MOPA configuration. *Opt. Express* **2015**, *23*, 5485–5490. [[CrossRef](#)] [[PubMed](#)]
16. Ma, P.F.; Huang, L.; Wang, X.L. High power broadband all fiber super fluorescent source with linear polarization and near diffraction-limited beam quality. *Opt. Express* **2016**, *24*, 1082–1088. [[CrossRef](#)] [[PubMed](#)]
17. Cao, J.; An, Y.; Pan, Z.; Huang, Z.; Yu, Y.; Guo, S.; Chen, J. A 186-Watt all-fiber single-stage super-fluorescent source. In Proceedings of the CLEO: Science and Innovations 2016, San Jose, CA, USA, 5–10 June 2016; p. SM4Q.7.
18. Li, Z.; Li, G.; Gao, Q.I.; Wu, P.; She, S.F.; Wang, Z.L.; Huang, N.; Sun, C.; Gao, W.; Ju, P.; et al. Kilowatt-level tunable all-fiber narrowband super-fluorescent fiber source with 40 nm tuning range. *Opt. Express* **2020**, *28*, 10378–10385. [[CrossRef](#)] [[PubMed](#)]
19. Song, J.; Wu, H.S.; Ren, S.; Liu, W.; Ma, P.F.; Xiao, H.; Zhou, P. Comparisons of kilowatt Yb-Raman fiber amplifiers employing a super-fluorescent fiber source and fiber oscillator. *Opt. Express* **2021**, *29*, 22966–22972. [[CrossRef](#)] [[PubMed](#)]
20. Perevezentsev, E.; Poteomkin, A.; Khazanov, E. Comparison of phase-aberrated laser beam quality criteria. *Appl. Opt.* **2007**, *46*, 774–784. [[CrossRef](#)] [[PubMed](#)]
21. Siegman, A.E. New developments in laser resonators. *Proc. SPIE* **1990**, *1224*, 2–14.
22. Siegman, A.E. How to (maybe) measure laser beam quality. In *DPSS (Diode Pumped Solid State) Lasers: Applications and Issues*; Vol. 17 of OSA Trends in Optics and Photonics, Paper MQ1; Dowley, M., Ed.; Optical Society of America: Washington, DC, USA, 1998.
23. Borgentun, C.; Bengtsson, J.; Larsson, A. Full characterization of a high-power semiconductor disk laser beam with simultaneous capture of optimally sized focus and farfield. *Appl. Opt.* **2011**, *50*, 1640–1649. [[CrossRef](#)] [[PubMed](#)]

Disclaimer/Publisher’s Note: The statements, opinions and data contained in all publications are solely those of the individual author(s) and contributor(s) and not of MDPI and/or the editor(s). MDPI and/or the editor(s) disclaim responsibility for any injury to people or property resulting from any ideas, methods, instructions or products referred to in the content.